PERIODIC SOLUTIONS OF THE GINZBURG–LANDAU EQUATION

Lawrence SIROVICH and Paul K. NEWTON*
Division of Applied Mathematics, Brown University, Providence, RI 02912, USA

Spatially periodic solutions to the Ginzburg–Landau equation are considered. In particular we obtain: criteria for primary and secondary bifurcation; limit cycle solutions; nonlinear dispersion relations relating spatial and temporal frequencies. Only relatively simple tools appear in the treatment and as a result a wide range of parameter cases are considered. Finally we briefly treat the case of spatial bifurcations.

1. Introduction

The Ginzburg–Landau equation [1]

$$\left(\frac{\partial}{\partial t} - \nu\frac{\partial}{\partial x} - \lambda\frac{\partial^2}{\partial x^2}\right)A = \left((R - R_c) - \beta|A|^2\right)A$$

is of wide current interest. This equation, which results from non-linear stability theory, governs the evolution of the (slowly varying) complex amplitude coefficient, A, of a neutral plane wave, $\exp[-i(\omega_c t + k_c x)]$. The subscript c signifies a critical value in a typical stability analysis, a brief description of which is given below. For the moment we mention that β and λ are complex, ν, a group speed, is real as is the control parameter, R. For diverse fluid flows this equation describes the passage ($R < R_c \rightarrow R > R_c$) of a base flow to a new state. In particular it occurs in the study of the Bénard problem [2], the Taylor problem [3], Tollmien–Schlichting waves [4, 5] and gravity waves [6, 7]. In other connections it arises in the study of chemical reactions [9, 10] and semi-conductors [11].

Typically the dispersion relation which results from the linear part of this equation gives a parabolic fit to the exact neutral stability curve in the neighborhood of the critical point (ω_c, k_c, R_c). The spatially independent form was suggested by Landau [12] on heuristic grounds to account for transition to a bifurcated state for supercritical

flows ($\text{Re}\,\beta > 0$). Stuart [13] and Watson [14] later in the context of parallel flows supplied formal derivations leading to the cubic term. The actual derivation of the Ginzburg–Landau equation was given by Benny and Roshkes [6] for Stokes waves and by Newell and Whitehead [2] in context of the Bénard problem. Davey [15] and Newell [16] later gave a formal derivation of this amplitude equation in a more general context (see also [4, 17–19]). An important feature of the Ginzburg–Landau equation is that it includes the resonance effects of Eckhaus [20] and Benjamin and Feir [21–22] while also including a continuous band of modes. Stuart and DiPrima [23] give an account of this as well as the early history.

As we have outlined the Ginzburg–Landau equation describes the non-linear transition from a base state to a new state as the relevant control parameter passes its critical value. At the lowest order it produces the new state and predicts whether the new state is stable or not. Thus for example it describes transformation from quiescent to convective heat transfer in the Bénard problem as the Rayleigh number is varied [24–27], and transition from circumferential to toroidal flow in Taylor–Couette flow as the Taylor number is varied [3]. Generally one has some latent destabilizing motion, held in check by a restoring or resistive force, which is released as the control parameter passes its critical value. For supercritical flows such as the Bénard and Taylor problems

*Present address: Department of Mathematics, Stanford University, Stanford, CA 94305, USA.

a new regular state can be expected, while for subcritical cases, such as parallel flows, bursting solutions are expected.

The above discussion underlines the idea that the neighborhood of a critical point is rich in phenomena. Therefore the Ginzburg–Landau equation should give rise to an equally rich structure of solutions independently of its detailed derivation. This lies at the heart of a wide variety of numerical experiments undertaken on the Ginzburg–Landau equation in recent times [8, 28–33]. These studies all indicate the presence of chaotic behavior. Indeed this was the main focus of the work of Kuramoto [8] and Nozaki and Bekki [33], who followed the evolution of smooth regular initial data and of Spiegel and Bretherton [31] and Deissler [32] who tracked the progress of initial noise. Our interest in this paper lies closer to the approach of Moon et al. [28–29] and Keefe [30] who follow the detailed *route to chaos* which is of current interest.

The form of the Ginzburg–Landau equation given above can be considerably reduced. Transformation to a frame moving with the group speed ν eliminates that term and a relatively straightforward change of variables reduces the equation to the form [34]

$$i\psi_t + (1 - ic_0)\psi_{xx} = i\rho\psi - (1 + i\rho)|\psi|^2\psi;$$
$$0 \le c_0^2 \le c_1, \quad \rho = c_0/c_1. \quad (1)$$

In the process of obtaining (1) we have excluded the subcritical case. (As is easily seen the spatially independent form of (1) for $\rho > 0$, has a bifurcated solution.) In the limit $c_0 \downarrow 0$ the cubic Schrödinger equation is obtained while for $c_0 \uparrow \infty$ (with a time renormalization) the Newell–Whitehead equation [2] is obtained. The conditions on c_0 and c_1 are equivalent to Newell's criterion that the spatially periodic case be unstable, which is the case of interest to us.

A simple solution to (1) is the Stokes solution

$$\psi = e^{it}. \quad (2)$$

In the numerical experiments a spatially perturbed form of (2) is followed in time. The Stokes equation is relevant to a gravity wave analysis where it relates frequency to amplitude changes. On the other hand (2) is not a solution of the Newell–Whitehead equation and is not, therefore, of general physical significance. On the other hand the dynamics which follows is of intrinsic interest and the hope is that it is representative.

In the numerical experiments one typically considers a 'box' in the sense that $2\pi/q$ spatially periodic initial disturbances are considered. Thus even after the application of the normalization contained in (1), the problem still depends on three parameters (c_0, c_1, q). The numerical calculations in [2, 28, 29, 30] use a spectral method in which the complex amplitude ψ is expanded in as much as 32 harmonics of q. This leads to relatively long machine calculations especially when fine detail is sought (e.g. distinguishing between one and two torus motions).

Sampling of the parameter space, (q, c_0, c_1) usually proceeds in two ways. Thus Kuramoto [8] fixes q and samples the coupling parameters (c_0, c_1) while Moon et al. [28, 29] and Keefe [30] fix these coupling parameters and vary the box size, q. Broadly speaking these numerical experiments have demonstrated that (1) leads to motions on low dimensional tori (limit cycles, two-tori, three-tori) as well as chaos. However, only a relatively small set of parameter space has been sampled. As we show the sparseness of sampled cases has produced several erroneous conclusions. Keefe [30] who recognized this problem carefully examined a relatively small set, $c_1 = 1$, $c_0 = 0.25$, $1.3 > q \ge 0.6$ and as q decreased found the following sequence of states: limit cycle; two torus; chaos; two-torus; chaos; two-torus; limit cycle, which certainly attests to the rich variety of phenomena produced by (1).

In the following we employ a variety of analytical tools to simplify the calculations and as a result are able to cover wide ranges of parameter space. For example, the construction of limit cycle solutions is reduced to a few seconds of comput-

ing time. This results in non-linear dispersion relations over virtually continuous ranges of parameter space. Methods based on Floquet theory [35] are then used to determine curves of secondary bifurcation. (Prior to the present study only one point of secondary bifurcation had been obtained [30].) This analysis also demonstrates that the cubic Schrödinger limit is qualitatively different than previously supposed.

Finally we show a close connection between these stability questions and the idea of spatial bifurcations. In fact we show that for a given set of coupling parameters (c_0, c_1) there is an infinite sequence of intervals in q-space corresponding to boxes of increasing size for which limit cycle solutions exist. This in turn suggests the possibility that the sequence of events found by Keefe is infinitely repeated in ever decreasing intervals of q-space.

A preliminary account of these results has already been reported [36].

2. Limit cycle solutions

As was shown in [34], eq. (1) possesses limit cycle solutions in the form of steady state oscillations

$$\psi_0 = \phi(x)\exp(i\Omega t). \tag{3}$$

The complex amplitude ϕ therefore satisfies

$$(1 - ic_0)\phi_{xx} = (\Omega + i\rho)\phi - (1 + i\rho)|\phi|^2\phi \tag{4}$$

and the condition of periodicity,

$$\phi(x + 2\pi/q) = \phi(x). \tag{5}$$

It is clear from inspection that: *eq. (4) supports both odd and even solutions.* In order to compare our results with Moon et al. [28, 29] and Keefe [30] we adopt their restriction to even solutions,

$$\phi(-x) = \phi(x). \tag{6}$$

We observe that in general: *equations of the form*

$$\phi_{xx} = f(\phi, \phi^*), \tag{7}$$

of which (4) is a special case, under transformation to first order form

$$\begin{aligned} U + iV &= \phi, \\ P + iQ &= \phi_x, \end{aligned} \tag{8}$$

defines a volume-preserving flow. (The extension of this statement to higher order differential equations is immediate.) To show volume preservation [37] we must show

$$\frac{\partial U_x}{\partial U} + \frac{\partial V_x}{\partial V} + \frac{\partial P_x}{\partial P} + \frac{\partial Q_x}{\partial Q} = 0 \tag{9}$$

which is immediately seen to be true. Thus if zero subscripts denote initial conditions then

$$\frac{\partial(U, V, P, Q)}{\partial(U_0, V_0, P_0, Q_0)} = 1, \tag{10}$$

i.e. the functional determinant is unity. It is in this form that the volume preserving property will be applied.

Solutions of (4) are invariant under multiplication by a constant of unit magnitude, i.e. for θ_0 a real constant, $\phi \exp(i\theta_0)$ is also a solution of (4) if ϕ is a solution. This suggests that the fourth order equation (4) can be reduced by one order and for this purpose it is convenient to represent ϕ in the form

$$\phi = r^{1/2}\exp\left(i\int_0^x v(x)\,dx\right), \tag{11}$$

where r and v are real functions. Direct substitution then shows that these satisfy

$$\begin{aligned} r_x &= 2ur, \\ v_x &= \frac{(c_0\Omega + \rho)}{(1 + c_0^2)} - \frac{(c_0 + \rho)}{(1 + c_0^2)}r - 2uv, \\ u_x &= \frac{(\Omega - c_0\rho)}{(1 + c_0^2)} - \frac{(1 - c_0\rho)}{(1 + c_0^2)}r - u^2 + v^2, \end{aligned} \tag{12}$$

where the first equation of (12) defines u. It is of interest to note that: *the flow defined by* (12) *is volume preserving in* (r^2, u, v)-*space*. This follows directly from the observation that

$$\frac{\partial (r^2)_x}{\partial r^2} + \frac{\partial v_x}{\partial v} + \frac{\partial u_x}{\partial u} = 0. \tag{13}$$

Corresponding to the even, (6), periodic, (5), solution to (4) we have that u and v are odd while r is even. It therefore follows that we can take,

$$u(0) = 0 = v(0), \quad r(0) = R_0. \tag{14}$$

In the procedure we follow to determine ϕ, the frequency Ω is prescribed and the corresponding wavenumber q (see (5)) determined. The trajectory generated by (12) is then viewed as it crosses the Poincaré section, $u = 0$. For a proper choice of the initial value the trajectory will cross the $u = 0$ Poincaré plane with a value $v = 0$ after a half cycle (at a different value of r). This is used as the basis of a Newton iteration scheme for the determination of the correct initial value (14). If we denote the actual value of v at the Poincaré section by $\hat{v}(R)$ (R the guessed value of R_0) then

$$R_0 = R - \hat{v}(R)/\hat{v}_R(R), \tag{15}$$

defines the iteration procedure, where $\hat{v}_R = \partial \hat{v}/\partial R$. It follows from (11) that this derivative satisfies the variational equation

$$\frac{\mathrm{d}}{\mathrm{d}x} \begin{bmatrix} r_R \\ v_R \\ u_R \end{bmatrix} = \begin{bmatrix} 2u & 0 & 2r \\ \dfrac{-(c_0 + \rho)}{(1 + c_0^2)} & -2u & -2v \\ \dfrac{-(1 - c_0\rho)}{(1 + c_0^2)} & 2v & -2u \end{bmatrix} \begin{bmatrix} r_R \\ v_R \\ u_R \end{bmatrix}. \tag{16}$$

The system, (16) (with initial data $(r_R, v_R, u_R) = (1, 0, 0)$) is solved simultaneously with (11) until the Poincaré section is reached. (We use Hénon's trick [38] for exactly landing on the Poincaré section.) A new value of R is then determined by

(15) and as a result of the quadratic convergence of Newton's method only a few iterations are required.

A typical limit cycle obtained in this way is displayed in fig. 1. In fig. 2 we exhibit a variety of dispersion relations

$$\Omega = \Omega(q; c_0; c_1) \tag{17}$$

obtained by this method. The procedure is extremely fast and a wide range of parameter space can be covered in relatively short times.

As a simple linear stability analysis on (1) shows, the Stokes solution (2) becomes unstable when

$$q^2 < q_0^2 = \frac{2(1 - c_0^2/c_1)}{(1 + c_0^2)} \tag{18}$$

(see refs. 16, 23, 34). It might then be supposed that (3) would follow from a perturbation analy-
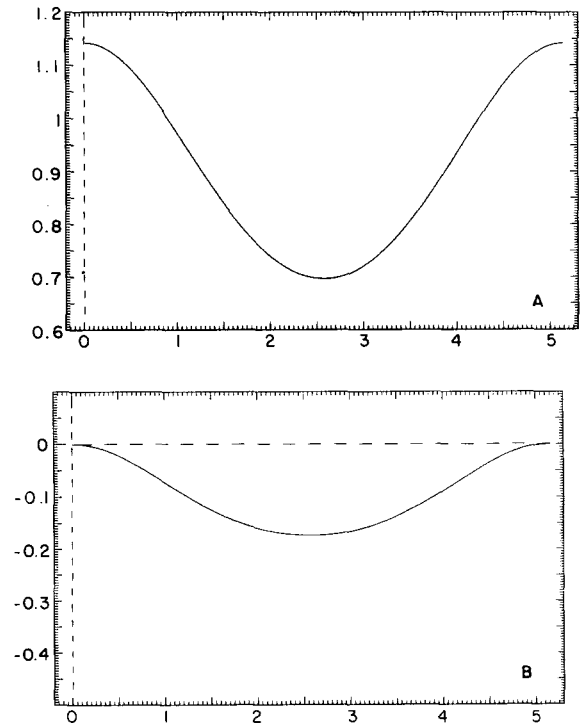

Fig. 1. Periodic solution for parameter values $c_0 = 0.25$, $c_1 = 1$, $\Omega = 0.9$, $\epsilon = 0.52$, $q = 1.22$. A) real spatial part; B) imaginary spatial part.
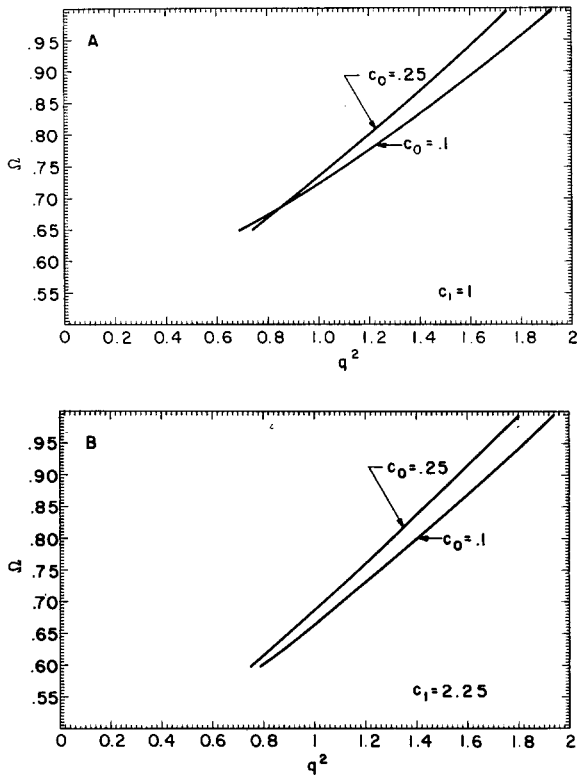
Fig. 2. Dispersion relations Ω vs. q^2. A) $c_1 = 1$; $c_0 = 0.1$, $c_0 = 0.25$; B) $c_1 = 2.25$; $c_0 = 0.1$, $c_0 = 0.25$.

sis. Such an approach, using the parameter $q_0^2 - q^2$, is considered in [34], and extremely good agreement with the numerical solutions is obtained.

3. Stability

As is known from the many numerical experiments the next step in the route to chaos is instability of the limit cycle solution, and the subsequent establishment of two torus motion. We now develop a method for the determination of the onset of secondary instability by methods drawn in part from Floquet theory [35].

In keeping with earlier notation we express the perturbed form of the limit cycle solution by

$$\psi(x, t) = (\phi(x) + \Psi(x, t)) \exp(i\Omega t). \tag{19}$$

In the infinitesimal limit it follows from (1) that the perturbation, Ψ satisfies the variational equation

$$\partial_t \Psi = L\Psi = z_1\Psi + z_2\Psi_{xx} + z_3(2|\phi|^2\Psi + \phi^2\Psi^*), \tag{20}$$

where

$$z_1 = \rho - i\Omega, \quad z_2 = c_0 + i, \quad z_3 = i - \rho.$$

It is therefore of interest to consider the eigenvalue problem,

$$L\Psi = \lambda\Psi. \tag{21}$$

Since our primary interest is in the question of stability we will be interested in the passage of λ across the imaginary axis. We will verify a posteriori that it does this along the real axis, i.e. by *exchange of stability*. Therefore for present purposes it will suffice if λ is taken real.

Since the steady state oscillation solution, ψ_0, satisfies the Ginzburg–Landau equation (1) it is a straightforward exercise to see that the space and time derivatives of ψ_0 individually satisfy the eigenfunction equation (21) with the eigenvalue, λ, set to zero. In particular we will write these two known eigenfunctions as

$$\lambda = 0, \quad \Psi_1 = i\phi, \tag{22}$$

$$\lambda = 0, \quad \Psi_2 = \phi_x. \tag{23}$$

It should be observed that the second solution Ψ_2 is an odd function while the first, Ψ_1, is even.

Several aspects of the problem become clearer if the problem is put in first order form. To do this we again use (8), which in the present instance is written as

$$u + iv = \Psi, \tag{24}$$

$$\mu + i\nu = \Psi_x. \tag{25}$$

If we use the notation

$$\boldsymbol{u} = (u, v, \mu, \nu), \tag{26}$$

the eigenvalue problem then may be written as

$$\lambda \mathbf{M} u + \left(\frac{\mathrm{d}}{\mathrm{d}x} - \mathbf{F} \right) u = 0, \qquad (27)$$

where the matrices appear in 2×2 blocks,

$$\mathbf{F} = \begin{pmatrix} 0 & 1 \\ \mathbf{f} & 0 \end{pmatrix}, \quad \mathbf{M} = \frac{1}{1 + c_0^2} \begin{bmatrix} 0 & & 0 \\ -c_0 & -1 & \\ 1 & -c_0 & 0 \end{bmatrix}. \qquad (28)$$

The details of the 2×2 $2\pi/q$-periodic matrix $\mathbf{f}$ are given in appendix A. *In order for instability to occur, the eigenvalue λ of* (21) *must pass through zero. Thus in view of* (22)–(23) *the algebraic multiplicity of $\lambda = 0$ must then be at least three. (As will be seen, the geometric multiplicity is two.)* To prove this we introduce the Jacobi matrix

$$\mathbf{U} = (u_a, u_b, u_c, u_d), \qquad (29)$$

with column vectors $\partial u/\partial a$, $\partial u/\partial b$, $\partial u/\partial c$, $\partial u/\partial d$. The constants a, b, c, d refer to initial values,

$$u(x = 0) = (a, b, c, d). \qquad (30)$$

It then follows that if $\lambda = 0$ in (27) then

$$\frac{\mathrm{d}}{\mathrm{d}x} \mathbf{U} = \mathbf{FU}. \qquad (31)$$

As we mentioned in the previous section a direct consequence of the volume preserving property (9) is that the functional determinant is unity (10), and hence

$$\det \mathbf{U} = 1. \qquad (32)$$

In particular, the Floquet matrix [35]

$$\mathbf{F} = \mathbf{U}(x = 2\pi/q), \qquad (33)$$

has this property, i.e.

$$\det \mathbf{F} = 1. \qquad (34)$$

Further detail and properties of $\mathbf{F}$ are given in appendix B.

The $2\pi/q$-periodic solutions of (27) with $\lambda = 0$, must satisfy initial data u_0 such that

$$u(2\pi/q) = \mathbf{U}(2\pi/q) u_0 = \mathbf{F}u_0 = u_0. \qquad (35)$$

Hence, u_0 must be an eigenvector of $\mathbf{F}$ corresponding to a unit eigenvalue, $\Lambda = 1$. (Eigenvalues of the Floquet matrix will be denoted by Λ.) Two such eigenvectors are known to us from (22) and (23). In particular, corresponding to Ψ_1 we have

$$u_1 = \left(0, R_0^{1/2}, 0, 0 \right), \qquad (36)$$

where we recall that $\phi(0) = R_0$, and corresponding to Ψ_2:

$$u_2 = \left(0, 0, \phi_{r_x}(0), \phi_{i_x}(0) \right), \qquad (37)$$

where ϕ_r and ϕ_i refer to the real and imaginary parts of ϕ. Both u_1 and u_2 satisfy the eigenvector condition (35).

If the geometric multiplicity of $\lambda = 0$ is to be more than two, then the Floquet matrix must have at least one more unit eigenvalue. To pursue this possibility let us first note that as a result of (34) the two remaining eigenvalues of $\mathbf{F}$ are reciprocals of one another. In fig. 3 we show the result of such a search. We plot there the typical evolution of these two remaining eigenvalues as we decrease the frequency Ω. The eigenvalues move monotonically and as mirror images around the unit circle until a critical value is reached at which $\Lambda = -1, -1$ (we remark without further comment for the moment that this implies the presence of spatial period doubling). For frequencies below this value the eigenvalues are real reciprocals and as a result, the Newton iteration of the last section starts to lose its effectiveness. In any event, in no instance does another eigenvalue to (33) become unity. Therefore instability does not appear according to this scenario.

If instability is to occur there is only one other scenario open to us. Namely that the unstable eigenfunction, as $\lambda \to 0$, becomes proportional to ψ_1, the known even eigenfunction. In a manner of speaking it makes the passage across the imagi-
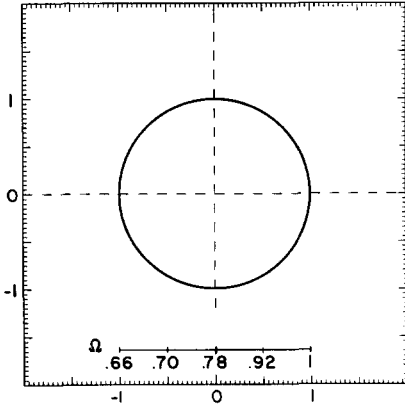
Fig. 3. Complex λ plane. Evolution of eigenvalues vs. Ω.

nary axis invisibly, disguised as ψ_1. In this event the geometric multiplicity of $\lambda = 0$ is two.

To pursue this possibility denote by Ω_0 the value of Ω at which this occurs. Then in the neighborhood of this point we write

$$\hat{\Omega} = \Omega_0 + \epsilon \qquad (38)$$

and

$$\hat{\psi} = \Psi_1(x : \hat{\Omega}) + \epsilon p(x), \qquad (39)$$

where ϵ is a measure of closeness to the transition point, and $p(x)$ is the perturbation to the eigenfunction. We also write the corresponding eigenvalue as

$$\lambda_1 = k\epsilon, \qquad (40)$$

where k is a constant. (Generically $\lambda_1 = \mathcal{O}(\epsilon^{1/2})$ but since the eigenvalue must actually cross the origin, $\lambda_1 = \mathcal{O}(\epsilon)$.) If these forms are substituted into (21) we find

$$Lp = (\rho - i\Omega_0)p + (i + c_0)p_{xx}$$
$$+ (i - \rho)(2|\phi|^2 p + \phi^2 p^*) = \psi_1 = i\phi, \qquad (41)$$

where the unimportant factor k has been absorbed in p. (In obtaining (41) we have used the fact that $L\Psi_1(x; \Omega_0) = 0$.) Eq. (41) is to be solved subject to the condition that p is $2\pi/q$-periodic

and even. It is important to note that L is not a self-adjoint operator and thus p is the generalized eigenfunction such that

$$L^2 p = 0. \qquad (42)$$

The condition for the determination of

$$\Omega_0 = \Omega_0(c_0, c_1), \qquad (43)$$

the frequency at which secondary instability sets in arises from the Fredholm condition that $i\phi$ be orthogonal to the null space of the adjoint of L.

In the actual calculation of (43) an equivalent though different algorithm was used. We considered the first order system corresponding to (41) which can be written in the form

$$\frac{dw}{dx} = Fw + h, \qquad (44)$$

where

$$h = \left(0, 0, (\phi_r - c_0\phi_i), (\phi_i + c_0\phi_r)/(1 + c_0^2)\right). \qquad (45)$$

A particular solution of (44), H, is constructed with the initial data

$$H(x = 0) = (0, 0, 0, 0). \qquad (46)$$

The general solution to (44) can therefore be represented in terms of the solution U to (31) by

$$w = Uw_0 + H, \qquad (47)$$

with the constant vector w_0 still to be determined. Since the proposed solution is to be periodic, we must have

$$w(2\pi/q) = w_0 = U(2\pi/q)w_0 + H(2\pi/q)$$
$$= Fw_0 + H_0 \qquad (48)$$

and the condition on w_0 is that

$$(1 - F)w_0 = H_0. \qquad (49)$$

The null space of $(1 - F)$ is always two dimensional since the Floquet matrix, F has two unit
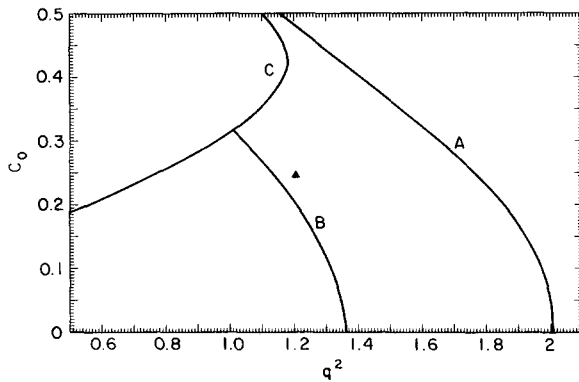
Fig. 4. c_0 vs. q^2 plane, $c_1 = 1$. A) primary transition curve; B) secondary transition curve; C) spatial period doubling curve.

eigenvalues. The condition that w_0 can be found is therefore that H_0 be orthogonal to the left null space (two dimensional) of $(1 - F)$. (Due to parity considerations we always can construct one such left null vector to be orthogonal to H_0.) For a distinguished value of Ω, (43), we find this condition to be satisfied. In fig. 4 the curve B gives the locus of secondary bifurcation for the case $c_1 = 1$ and c_0 varying. We also indicate with a filled triangle the one reliable numerical value of secondary transition as found by Keefe [30]. In-as-much-as Keefe made a relatively fine sampling of cases in the vicinity of this one value one can wonder why the agreement is not better. Since Keefe solved the initial value problem for (1) it was necessary for him to carry such computations to extreme lengths to decide if the solution resided on a one or two torus. Thus accumulated round off and truncation error is a possible cause. Another, less likely, possibility is that the thirty-two harmonics carried by Keefe in his spectral method is insufficient.

4. Discussion

As remarked earlier the cubic Schrödinger equation results from (1) under the limit $c_0 \downarrow 0$. From fig. 4 we observe that the secondary instability curve, B, strikes the $c_0 = 0$ axis at roughly $q^2 \approx$ 1.35. This contradicts the picture presented by

Moon et al. [28, 29] who shows this curve meeting the point $c_0 = 0$, $q = q_0$. Moon as a result of the initial value problem he solves found two-torus motions on the $c_0 = 0$ axis and mistakenly concluded that one torus motion could not be found. The cubic Schrödinger equation is an integrable Hamiltonian system and thus supports limit cycle, two torus, as well as motions of higher genus. Therefore the surface followed by a solution depends sensitively on initial data. In fact it would be remarkable if the initial data chosen in [28, 29] exactly landed on a two torus.

As noted earlier, the iteration scheme used to obtain the limit cycle solution ceases to be effective beyond the point when the additional eigenvalues reach $\lambda = -1$, for after this, one solution grows exponentially. For present purposes it was not felt necessary to modify the analysis to capture the limit cycle solutions beyond this range. The appearance of an eigenvalue $\lambda = -1$ signals the presence of nearby solutions which exhibit spatial period doubling. The locus of the period doubling curve is shown as, C, in fig. 4 and is seen to cut across the secondary bifurcation plot at $c_0 \approx 0.32$.

It is of interest to consider the case of spatial period doubling. In fig. 5 we show the Poincaré section, $u = 0.0$ for $c_0 = 0.25$, $c_0 = 1$ and $\Omega = 0.66$ with initial conditions slightly away from the cor-
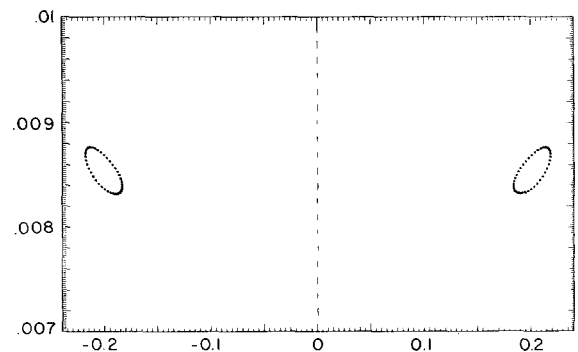

Fig. 5. Poincaré $u = 0$ section ($u_x > 0$); $c_1 = 1$, $c_0 = 0.25$, $\Omega = 0.7805$. The section for $u_x < 0$ gives two closed curves straddling the $v = 0$ axis.

responding limit cycle value. As is seen a two torus motion results. The *center* of the ellipses in fig. 5 correspond to a spatially period-doubled limit cycle solution. We do not know the value of q corresponding to this limit cycle but we do know that it is roughly half the q value which can be read off of fig. 2. In fact as this discussion shows there is a window of values of Ω and a corresponding window of q values which give spatially period doubled limit cycles.

The argument just given applies equally to all Ω which lead to λ's of the form

$$\lambda = \exp(2\pi i/N), \quad N = 2, 3, \ldots . \quad (50)$$

As an illustration we show in fig. 6 a two torus motion for $\Omega = 0.7805$ which lies near the value of Ω at which $\lambda = \pm i$. In this instance the center of any of these ellipses corresponds to a period quadrupled limit cycle. Again the remark about a window of such values being present is applicable as it is for all cases corresponding to (50). Thus it follows that there are an infinite succession of zones in which limit cycle behavior exists. It would seem likely that these interleave two-torus zones followed by chaos as found by Keefe [30] – each zone diminishing in width as $q \to 0$ is approached. However, in the absence of actual calculations this is just speculation.
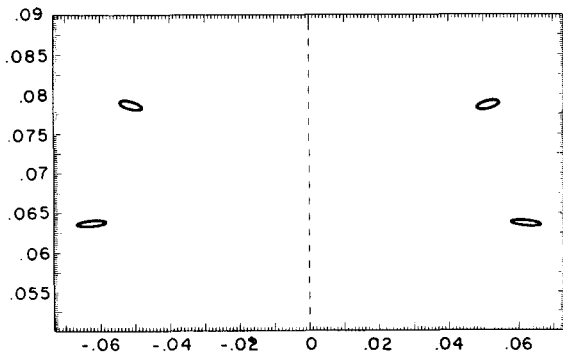

Fig. 6. Poincaré $u = 0$ section ($u_x > 0$); $c_1 = 1$, $c_0 = 0.25$, $\Omega = 0.66$. The section for $u_x < 0$ gives four closed curves straddling the $v = 0$ axis.

Appendix A

The coefficient matrix **F** is given by

$$\mathbf{F} = \begin{pmatrix} 0 & 1 \\ \mathbf{f} & 0 \end{pmatrix}, \quad (A.1)$$

where

$$\mathbf{f} = \begin{pmatrix} \alpha_{11} & \alpha_{12} \\ \alpha_{21} & \alpha_{22} \end{pmatrix}, \quad (A.2)$$

$$\alpha_{11} = -\frac{1}{(1 + c_0^2)} \left\{ (c_0\rho - \Omega) + 3\phi_r^2(1 - c_0\rho) \right.$$
$$\left. + \phi_i^2(1 - c_0\rho) - 2c_0\phi_r\phi_i\left(1 + \frac{1}{c_1}\right) \right\}, \quad (A.3)$$

$$\alpha_{12} = -\frac{1}{(1 + c_0^2)} \left\{ c_0\left(\Omega + \frac{1}{c_1}\right) - c_0\phi_r^2\left(1 + \frac{1}{c_1}\right) \right.$$
$$\left. - 3c_0\phi_i^2\left(1 + \frac{1}{c_1}\right) + 2\phi_r\phi_i(1 - c_0\rho) \right\}, \quad (A.4)$$

$$\alpha_{21} = -\frac{1}{(1 + c_0^2)} \left\{ -c_0\left(\Omega + \frac{1}{c_1}\right) + 3c_0\phi_r^2\left(1 + \frac{1}{c_1}\right) \right.$$
$$\left. + c_0\phi_i^2\left(1 + \frac{1}{c_1}\right) + 2\phi_r\phi_i(1 - c_0\rho) \right\}, \quad (A.5)$$

$$\alpha_{22} = -\frac{1}{(1 + c_0^2)} \left\{ (c_0\rho - \Omega) - \phi_r^2(c_0\rho - 1) \right.$$
$$\left. - 3\phi_i^2(c_0\rho - 1) + 2c_0\phi_r\phi_i\left(1 + \frac{1}{c_1}\right) \right\}. \quad (A.6)$$

Appendix B

The 4×4 matrix $\boldsymbol{F}$ has the following properties:

Property 1.

$$F_{12} = F_{32} = F_{42} = 0, \quad F_{22} = 1. \quad (B.1)$$

This follows from the exact solution Ψ_1, (22). Specifically, if T denotes the period of a solution $\mathbf{U}$ to (31), then

$$\mathbf{U}(T) = \mathbf{F}\mathbf{U}(0). \tag{B.2}$$

In vector form, the exact solution (22) is

$$u_1 = \begin{bmatrix} -\phi_1 & \phi_r & -\phi_{i_x} & \phi_{r_x} \end{bmatrix}. \tag{B.3}$$

Hence:

$$u_1(0) = \begin{bmatrix} 0 & R_0^{1/2} & 0 & 0 \end{bmatrix}. \tag{B.4}$$

Using (B.4) and the fact that

$$u_1(0) = u_1(T), \tag{B.5}$$

gives the result.

Property 2.

$$\frac{F_{14}}{F_{13}} = \frac{F_{24}}{F_{23}} = K_1, \tag{B.6}$$

$$F_{33} = 1 + \frac{1}{K_1} F_{34}, \tag{B.7}$$

$$F_{43} = \frac{1}{K_1} (F_{44} - 1), \tag{B.8}$$

where

$$K_1 = -\phi_{r_x}|_{x=0}/\phi_{i_x}|_{x=0}. \tag{B.9}$$

This follows from the exact solution Ψ_2, (23). In vector form, this solution is

$$u_2 = \begin{bmatrix} 0 & 0 & \phi_{r_x} & \phi_{i_x} \end{bmatrix}. \tag{B.10}$$

Hence

$$u_2(0) = \begin{bmatrix} 0 & 0 & \phi_{r_x}|_0 & \phi_{i_x}|_0 \end{bmatrix}. \tag{B.11}$$

Using (B.2) and the fact that

$$u_2(0) = u_2(T), \tag{B.12}$$

gives the result.

References

[1] V.L. Ginzburg and L.D. Landau, Zh. Eksper. i. Teor. Fiz 20 (1950).
[2] A.C. Newell and J.A. Whitehead, J. Fluid Mech. 38 (1969) 279.
[3] S. Kogelman and R.C. DiPrima, Phys. Fluids 13 (1970) 1.
[4] K. Stewartson and J.T. Stuart, J. Fluid Mech. 48 (1971) 529.
[5] L.M. Hocking and K. Stewartson, J.T. Stuart, J. Fluid Mech. 51 (1972) 705–735.
[6] D.J. Benney and G.J. Roskes, Stud. Appl. Math. 48 (1969) 377–385.
[7] H. Hasimoto and H. Ono, J. Phys. Soc. Japan 33 (1972) 805.
[8] Y. Kuramoto, Progress of Theoretical Physics Supp. 64 (1978) 346.
[9] Y. Kuramoto and T. Yamada, Progress of Theoretical Physics 56 (1976) 670.
[10] Y. Kuramoto and S. Koga, Phys. Lett. A92 (1982) 1.
[11] M. Pavlik and G. Rowlands, J. Phys. C8 (1975) 1189.
[12] L.D. Landau, C.R. Acad. Sci. U.R.S.S. 44 (1944) 311.
[13] J.T. Stuart, J. Fluid Mech. 9 (1960) 353–370.
[14] J. Watson, J. Fluid Mech. 9 (1960) 371–389.
[15] A. Davey, J. Fluid Mech. 53 (1972) 769–781.
[16] A.C. Newell, in: Nonlinear Wave Motion, A.C. Newell, ed. (AMS, Providence, RI, 1974).
[17] C.G. Lange and A.C. Newell, SIAM J. Appl. Math. 27 (1974) 441–456.
[18] R.C. DiPrima, W. Eckhaus and L.A. Segel, J. Fluid Mech. 49 (1971) 705–744.
[19] J.D. Gibbon and M.J. McGuinness, Proc. R. Soc. Lond. A377 (1981) 185–219.
[20] W. Eckhaus, Studies in Nonlinear Stability Theory (Springer, Berlin, 1965).
[21] T.B. Benjamin, Proc. R. Soc. Lond. A299 (1967) 59–75.
[22] T.B. Benjamin and J.E. Feir, J. Fluid Mech. 27 (1967) 417–430.
[23] J.T. Stuart and R.C. DiPrima, Proc. Roy. Soc. Lond. Ser. A362 (1978) 27.
[24] A. Schlüter, D. Lortz and F. Busse, J. Fluid Mech. 23 (1965) 129.
[25] F. Busse, Proc. I.U.T.A.M. Symp. Inst. Cont. Syst., Herrenalb, (Springer, Berlin, 1971).
[26] F.H. Busse and J.A. Whitehead, J. Fluid Mech. 47 (1971) 305–320.
[27] F.H. Busse and R.M. Clever, J. Fluid Mech. 91 (1979) 319–335.
[28] H.T. Moon, P. Huerre and L.G. Redekopp, Phys. Rev. Lett. 49 (1982) 7.
[29] H.T. Moon, P. Huerre and L.G. Redekopp, Physica 7D (1983) 135.
[30] L. Keefe, Studies in Applied Math. 73 (1985) 91.
[31] C.S. Bretherton and E.A. Spiegel, Phys. Lett. A96 (1983) 3.
[32] R.J. Deissler, J. Stat. Phys. 40 (1985) 371–395.
[33] K. Nozaki and N. Bekki, Phys. Rev. Lett. 51 (1983) 24.
[34] P.K. Newton and L. Sirovich, Q.A.M. 43 (1986) 535–542.

[35] W. Magnus and S. Winkler, Hill's Equation (Interscience, New York, 1966).

[36] L. Sirovich and P.K. Newton, in: Stability of Time Dependent and Spatially Varying Flows. D.L. Dwoyer and M.Y. Hussani, eds. (Springer, New York, 1986).

[37] V.I. Arnold, Mathematical Methods of Classical Mechanics, (Springer, New York, 1978).

[38] M. Hénon, Physica 5D (1982) 412–414.